UNIVERSITY OF CALIFORNIA SAN DIEGO

Generation of a Mouse Model for Scar Production on the Retina

A thesis submitted in partial satisfaction of the requirements for the degree

Master of Science

in

Biology

by

Joseph Patrick Miller

Committee in Charge:

Richard Daneman, Chair
Brenda Bloodgood, Co-Chair
Eric Nudleman, Co-Chair
Lisa McDonnell

2019

The Thesis of Joseph Patrick Miller is approved, and it is acceptable in quality and form for publication on microfilm and electronically:

_____

_____
Co-Chair

_____
Co-Chair

_____
Chair

University of California San Diego

2019

DEDICATION

This manual is dedicated to my friends who keep me sane, my family who keep me down to Earth, and my many mentors who challenge and guide me down the path of enlightenment.

TABLE OF CONTENTS

Signature Page…… iii

Dedication……... iv

Table of Contents…… v

List of Figures ……..... vi

Abstract of the Thesis …… vii

Introduction……..... 1

Methods and Materials……... 6

Results…… 13

Discussion…….. 25

References…….. 30

LIST OF FIGURES

Figure 1: Collagen1a1-GFP expression at various postnatal timepoints in healthy mice.……13

Figure 2: Comparison between LOIR and traditional OIR protocols……..……. 14

Figure 3: Vascular comparison between LOIR mice retinas to P25 traditional OIR mice and LOIR age matched controls..…….…… 15

Figure 4: Collagen scar pathology in LOIR retinas…….…… 16

Figure 5: Collagen1a1-GFP positive cells per area in the Outer Plexiform and Superficial Layers of the retina..…… 17

Figure 6: Colocalization of various cellular markers with GFP positive cells in LOIR retinal sections…….. 18

Figure 7: Collagen scar pathology in dispase injected retinas…….. 19

Figure 8: Colocalization of various cellular markers with GFP positive cells in dispase injected retinal sections……...20

ABSTRACT OF THE THESIS

Reliable Retinal Scarring Disease Models in Mice

by

Joseph Patrick Miller

Master of Science in Biology

University of California San Diego, 2019

Richard Daneman, Chair
Brenda Bloodgood, Co-Chair
Eric Nudleman, Co-Chair

Wound healing is paramount for the survival of multicellular organisms, but this process can lead to scarring if left uncontrolled. Retinal scarring, in particular, occurs in many prevalent retinal diseases and is devastating as this pathology can lead to blindness. Unfortunately, little is

known about retinal scarring, such as the origin of cells producing the scar and the cellular mechanisms leading to scar formation. Understanding these elements behind scar production is vital in creating therapeutic targets that can prevent potential blindness in those affected by retinal scarring. Although there are many retinal disease models in mice, a reliable mouse retinal scarring model has not been established. In this study, I develop two scarring models in mice. One is a mouse model for the disease phthisis bulbi, which is characterized as a shrunken, non-functional eye that is caused by injury, inflammation or other infections. We induce these characteristic symptoms by injecting dispase, a neutral protease, into the eyes of mice, causing degradation of retinal tissue, eye shrinkage, and the production of scars. The other scarring model is termed as Long Oxygen Induced Retinopathy (LOIR), which is a more pathologically severe model of the traditional "Smith" OIR mouse model of retinopathy of prematurity. This newly developed scar producing model is induced by prolonging the exposure of highly concentrated atmospheric oxygen from the traditional "Smith" OIR model protocol of 5 days to 14 days. With these models, I answer what cell type(s) are producing scar tissue in the retina.

Introduction

The regenerative capability of all tissues is paramount in the survival of all multicellular organisms. Damage to tissues disrupts normal homeostatic function of that tissue, and it is imperative for regeneration to occur in order to recover homeostasis and proper tissue function. There are two stages of regeneration. First is a regenerative phase where old damaged tissue is replaced by new tissue [1]. In this phase, cellular repair mechanisms activate, which include immune cells migrating to the wound site and clearing debris, upregulation in wound-associated genes, fibroblast proliferation and migration to the wound site to provide structure and new extracellular matrix, and angiogenesis of blood vessels [2]. Second is a fibrotic phase, where this regeneration process becomes uncontrolled causing connective tissues to replace normal parenchymal tissue creating a scar, which can have devastating repercussions such as pain, tenderness, itching, and decreased organ function [1]. Scarring in this secondary phase is attributed to chronic inflammation and overactive cellular repairing mechanisms, leaving excessive extracellular matrix components in the damaged area [1]. It must be noted that these phases may not occur in wound repair. In some injuries, the regenerative phase may occur without the fibrotic phase initiating, which leads to optimal wound regeneration. Likewise, some injuries lead to only the fibrotic phase occurring without the regenerative phase initiating, which leads to suboptimal regeneration and functionally compromised tissues. In rare occurrences, neither phases occur. Furthermore, the formation of a scar can be more functionally compromising for certain tissues. For example, a scar on bone or skin does not compromise the function of the organ, but scarring in the liver can be debilitating as the scar leads to decreased function in the organ since scars and

extracellular matrix components replace and distort liver tissue, decreasing the amount of liver tissue that is available to store energy, digest food, filter blood, and fight infections [3,4].

Retinal scarring can be particularly devastating. Millions suffer from ocular diseases and injuries that lead to scarring such as proliferative vitreoretinopathy (PVR), retinopathy of prematurity (ROP), diabetic retinopathy (DR), and phthisis [5]. A common pathology of many of these diseases is the disruption of the blood retinal barrier, which is the combination of unique properties that cause the tight regulation of molecular movement between the blood and retina [6]. This disruption is caused by the development of new blood vessels, otherwise known as neovascularization, due to retinal tissue becoming hypoxic and requiring more oxygen for its metabolic needs. These new blood vessels lack the properties of the blood retinal barrier and leak ions, molecules, and cells into the retina. This leakage causes tissue damage and chronic inflammation which leads to retinal scarring, causing retinal traction and finally retinal detachment [5,7]. This is why it is particularly important to reiterate that retinal scarring directly causes retinal traction and thus causes retinal detachment. Therefore, decreasing scar deposition may save the retain and visual acuity in many retinal diseases and injuries. Retinal scarring is common in these retinal diseases due to the damage caused by neovascularization. Furthermore, scarring and retinal detachment treatment are therapeutically limited and highly invasive as they require surgical intervention [8]. Thus, the disease progression of retinopathies and ocular injuries need to be better understood in order for new therapies to develop [8].

The formation of a retinal scar is due to extracellular matrix secretion during injury, which consists largely of collagen proteins; type 1 collagen (collagen 1) specifically occurs in scar tissue as fibrils and is of interest in studies as a marker for fibrosis [9]. However, it is unclear what cell type is the source of the retinal scar tissue. Hiscott *et. al.* and Machemer *et. al.* suggest that retinal

fibrotic scars originate from retinal pigment epithelial (RPE) cells and adopt macrophage-like or fibroblast-like functions during retinal disorders; these cells then migrate to the site of injury forming a scar by producing collagen in the extracellular matrix [10,11]. Others suggest that Müller glia cells are activated as a consequence of neovascularization; upon activation, glial cells are thought to proliferate and extend processes to aid in the development of these new blood vessels [12]. These processes are thought to consequently extend to the vitreous where the glial cells can secrete extracellular matrix proteins and produce a scar (referred to as gliosis and a gliotic scar), causing traction, and finally retinal detachment [12]. Also, we know in peripheral tissues, fibroblasts are known to secrete extra cellular matrix proteins, like collagen 1 protein which is a marker for fibrosis, to help reform structural integrity of the damaged tissues. [13]. This makes this a cell type of interest in this study to see if the retinal scarring originates from fibroblasts in the retina. Or even perhaps even pericytes play a role in scarring since they help in angiogenesis of blood vessels in the central nervous system and may have properties that facilitate scar production. There is clearly a lack in consensus on what cell type, and by what cellular mechanism, produces scars in the retina. We aim to answer these questions.

In order to achieve these goals, we need to have a reproducible disease model in mice that reliably produces scarring on the retina. There are currently no widely used disease models in mice that reliably produce retinal scarring, and we aimed to try to develop two retinal scarring models. To produce an injury model that leads to scarring, we injected dispase, a neutral protease, into the vitreous in the eyes of mice [14]. Dispase injections are commonly used in rabbits as model for proliferative vitreoretinopathy, and it degrades surrounding tissue and produces a pathology similar to the disease pathology of phthisis in humans [15]. Cellular mechanisms will try to repair the degraded retina, leading to the production of extracellular matrix proteins and eventually the

formation of a scar. We also performed Oxygen Induced Retinopathy (OIR) on mice, a mouse model for human retinal ischemic diseases such as the above stated ROP [16]. When premature babies are born, their lives are threatened because their lungs are not developed enough to provide oxygen to the rest of their tissues for metabolic needs. Due to this, doctors provide oxygen treatment to these babies so their circulatory has enough oxygen to sustain bodily functions for the baby. However, the retinal vasculature, thereafter, stops developing since the retinal tissue has enough oxygen at this artificial concentration to sustain metabolic function without proper development of vasculature. Once removed from oxygen treatment, the retina becomes relatively hypoxic and develops new blood vessels, a process known as neovascularization, to bathe the retina with oxygen rich blood to sustain metabolic needs. As new abnormal vasculature forms and leaks ions and blood, the retina develops a ridge of scar tissue. Here scar tissue attaches to the vitreous and contracts, pulling the retina off the eye causing retinal detachment. This pathological process is retinopathy of prematurity [17]

If we are able to better understand the mechanisms behind scar formation, we can identify potential therapeutic targets that can potentially improve visual outcomes of ROP and other ischemic retinal diseases. We induce OIR based on Smith's *et. al.* protocol where we introduce increased atmospheric oxygen to mice, which leads to an initial phase of blood vessel depletion, then to a secondary neovascularization phase triggered by relative hypoxia once the mice are outside the high oxygen environment [16,18]. This model is outlined in figure 2. This classical "Smith model" for OIR does not lead to retinal scarring, however a more severe pathology that leads to retinal scarring may be induced by exposing young mice for a longer period of time [18,19]. Here, we designed specific exposure conditions to reliably reproduce scars in the retina based on the OIR model, which we reference as LOIR (Figure 2). We aim to use this new model

to answer what cells produce scarring in the retina, what are the molecular mechanisms behind scar formation in the retina, can we develop new therapeutic interventions to limit retinal scarring, and will limiting retinal scarring improve outcomes from retinal diseases.

Methods and Materials

Animals

Collagen1a1 GFP+ mice were obtained from David Brenner and maintained. These mice have a C57/Bl6 background.

Mouse model of Oxygen Induced Retinopathy (OIR)

The mouse OIR model was performed following Smith's *et. al.* a previously published protocol [16]. Briefly, pups and their nursing mothers were placed in a sealed 75% oxygen chamber (Biospherix, Parish, NY, USA) at postnatal day 7 (P7) and monitored daily. The mice were removed from the chamber at postnatal day 12 (P12) and placed in room air. Retinas from P12 (vaso-obliteration), P17 (neovascularization) and P25 (resolution) pups were used for further experiments and analysis.

Mouse model of Long Oxygen Induced Retinopathy (LOIR) (See Figure 2)

This mouse OIR model is based on information from Smith's *et. al.* a previously published protocol but was further optimized in this laboratory [18]. Pups and their nursing mothers were placed in a sealed 75% oxygen chamber (Biospherix, Parish, NY, USA) at postnatal day 2 (P2) and monitored daily. Every two days, the nursing mother mouse would be switched with a normoxic nursing mother mouse to minimize oxygen toxicity. The mice were removed from the chamber at postnatal day 16 (P16) and placed in room air. Retinas from P23 and P30 were used for further experiments and analysis.

Dispase Injections

This injury model is based on Frenzel's *et. al.* dispase injection protocol [14]. Ten-week-old mice were anesthetized with 500µl of Ketamine-Xylazine. Then 1 µl of 0.4 U/ml Neutral Protease (Dispase) (Worthington Biochemical Corporation, Lakewood, NJ, USA) dissolved in DPBS was injected in 10-week-old mice intravitreally with a 2.5 µl Hamilton syringe (Hamilton Company, Franklin, MA, USA). The injected mice were placed on a heating pad to wake up on. Eyes were enucleated two weeks post-injection and sectioned for immunostaining and imaging.

Reagents

1xDPBS used in the following experiments is Ca^{2+} and Mg^{2+}- free (Thermo Fisher Scientific, Waltham, MA, USA), unless specified otherwise.

4% PFA for tissue fixation was prepared from 32% PFA (Electron Microscopy Sciences, Hatfield, PA, USA) diluted in DPBS and kept at 4°C for maximum one week. Used PFA was disposed of in accordance to the Environment Health and Services (EH&S) guidelines.

Permeabilizing-blocking solution (Perm-Block) was prepared by dissolving 0.2% of bovine serum albumin powder (BSA – Sigma-Aldrich, St Louis, MO, USA), 0.3% of Triton X-100 [RD3] (Thermo Fisher Scientific, Waltham, MA, USA) and 5% of normal goat serum (NGS) (Life Technologies, Carlsbad, CA, USA) in DPBS.

Ketamine-Xylazine anesthesia solution was prepared by combining Ketamine at a final concentration of 100mg/kg (MWI/Vetone, Boise, ID, USAbrand) and Xylazine at a final concentration of 5mg/kg (MWI/Vetone, Boise, ID, USA) in sterile clinical-grade saline solution (MWI/Vetone, Boise, ID, USA).

30% Sucrose solution was prepared by dissolving sucrose (Sigma Aldrich, St. Louis, MO, USA) in 1xPBS.

Perfusion

Pups were anesthetized with 1-2ml of Ketamine-Xylazine (4mg/mL Ketamine and 0.6mg/mL Xylazine) 10 minutes before perfusion. The thoracic cavity of the mice was opened, the right atrium was clipped, and then we perfused the mice through the left ventricle of the heart with sterile DPBS for 2 minutes, at a speed of 4.5 ml/min, using the Dynamax RP-1 peristaltic pump (Mettler Toledo-Rainin, Oakland, CA). The mice were then perfused with 4% PFA for 8 minutes at the same speed of 4.5 ml/min. Finally, the mice were washed with DPBS for 1 minute. After perfusion, eyeballs were enucleated and post-fixed for 10 minutes in 4% PFA. One eyeball from a single mouse was placed in DPBS for retina dissection, and the other eye was placed in a 30% sucrose solution for sectioning.

Fluorescent dyes and Antibodies

The following fluorescent dyes and antibodies were used for immunostaining: primary antibody stains: BSL-rhodamine (Vector Laboratories Inc., Burlingame, CA, USA) or BSL-fluorescein (Vector Laboratories Inc., Burlingame, CA, USA) at a 1:500 dilution ratio; rabbit anti-collagen 1, goat anti-SOX9, and rat anti-CD31 (BD Biosciences, San Jose, CA, USA; Abcam, Cambridge, MA, USA) at a 1:500 dilution ratio. Secondary antibodies stains: donkey anti-rabbit A594, donkey anti-rat A594, and donkey anti-goat A594 (Life Technologies, Carlsbad, CA, USA) at a 1:500 dilution.

Retinal flat mounts and immunostaining

Pups that underwent dispase injections, OIR and long OIR, along with their respective same age normoxic controls, were euthanized, fixed, and had their eyeballs extracted. The eyeballs were placed in 4% PFA for 10 minutes, then rinsed once in DPBS. The whole retina was extracted in a 35x10mm petri dish (Becton Dickinson Labware, Franklin Lakes, NJ, USA) filled with DPBS under a dissecting microscope using two #5 forceps (FST by Dumont, Switzerland) and 27G needle (BD Biosciences, San Jose, CA, USA). Each retina was flattened on top of the same 35x10 mm petri dish. To flatten the retinal cup, short incisions were made using Vannas Spring Scissors (Fine Science Tools, Inc., Foster City, CA, USA). Once opened into a four leaf clover-like shape with the optic nerve at the center, one retina was placed per well in a 24-well plate (Corning, Corning, NY, USA) wrapped in an aluminum foil to prevent fluorescence decay, and blocked for 1 hour in Perm-Block (200µl/well) at room temperature on an orbital shaker. The Perm-Block was removed with a vacuum, and the retinas were placed in 200µl/well of fresh DPBS with primary antibodies added. The plate with the retinas moved to 4°C on a shaker overnight for primary antibody staining. The next day, primary antibodies were removed, and the retinas rinsed in 200µl/well of DPBS. After four washes, 10 minutes each, the retinas were placed in 200µl/well of DPBS with secondary antibodies were added. The plate, still wrapped in an aluminum foil, was then placed at 4°C on a shaker overnight. After the secondary antibody staining, retinas were rinsed four times for 15 minutes in 200µl/well of DPBS and laid flat on a 25x75x1mm microscopy slide (VWR, Randor, PA, USA), the inner side of the retina facing up. Retinas were mounted using the Vectashield mounting medium with DAPI (Vector Laboratories Inc., Burlingame, CA, USA), and covered with a thin glass coverslip (VWR, Randor, PA, USA). The slides were dried for 10 minutes in the dark, then sealed using nail polish (Electron Microscopy Sciences, Hatfield, PA, USA), the

imaged using a Zeiss Imager D2 fluorescence microscope (Carl Zeiss AG, Oberkochen, Germany) equipped with the AxioVision software (Carl Zeiss AG, Oberkochen, Germany).

Retinal Sectioning and immunostaining

Full eyeballs from the 30% sucrose solution were placed in a 10x10x5mm Cryomold (Sakura Finetek USA, Inc., Torrance, CA, USA) with Optimal Cutting Temperature (OCT) Compound (Sakura Finetek USA, Inc., Torrance, CA, USA) and frozen in an insulated container. Once the OCT was frozen with the eyeballs inside, the OCT was mounted in a cryostat in order to obtain 10μm sections of the retina. These sections were placed on a 25x75x1mm microscopy slide (VWR, Randor, PA, USA) for immunostaining. The sectioned retinas were circumscribed with an ImmEdge pen (Vector Laboratories, Inc. Burlingame, CA, USA) and were placed in Perm-Block for 30 minutes at room temperature. The slides were placed in a slide box to cover the retinas from the light to prevent fluorescence decay. Perm-Block was removed with a vacuum, and the retinas were placed in Perm-Block with primary antibodies overnight at 4℃. The next day, the Perm-Block with primary antibodies were removed with a vacuum and the retinas were washed three times for 10 minutes each was with 0.1% Triton-X 100 in DPBS. The retinas were then placed in 0.1% Triton-X 100 in DPBS with secondary antibodies added and left overnight to stain at 4℃. After the secondary antibody staining, retinas were rinsed four times for 15 minutes, twice with 0.1% Triton-X 100 in DPBS, then twice with just DPBS. Retinas were mounted using the Vectashield mounting medium with DAPI (Vector Laboratories Inc., Burlingame, CA, USA), and covered with a thin glass coverslip (VWR, Randor, PA, USA). The slides were dried for 10 minutes in the dark, then sealed using nail polish (Electron Microscopy Sciences, Hatfield, PA, USA) and

imaged, using a Zeiss Imager D2 fluorescence microscope (Carl Zeiss AG, Oberkochen, Germany) equipped with the AxioVision software (Carl Zeiss AG, Oberkochen, Germany).

ImageStudioLite Analysis

Retinal sections were analyzed in ImageStudioLite by circumscribing the entire retinal tissue with the freehand drawing tool and using a green color filter to analyze only green color in the images. I obtained GFP signal intensity and the area of retinal tissue in this software and normalized the signal intensity by the area in each retina analyzed.

ImageJ and Microsoft Excel Analysis [20]

Retinal sections were analyzed in ImageJ by using freehand selections to circumscribe the middle, surface, and scarring layer of the retina to obtain the area of each tissue image. The multipoint tool was used to count the number of GFP positive cells in each of those layers. The number of cells in each layer was normalized to the area of that layer. The normalized counts were averaged in RStudio, where a bar graph was created to compare P30 long OIR mice normalized counts to P30 controls in each layer. A two-tailed T-test was performed comparing the significance between each layer analyzed, and the standard deviation was calculated.

Prism for Data Analysis and Figure Production

GFP signal intensity and cell quantification data from Microsoft Excel were imported into Prism, where I then wrote a script to perform further statistical analysis in order to create the statistical figures in this experiment.

Biorender

This online program was used to illustrate the long OIR protocol in Figure 2.

Results

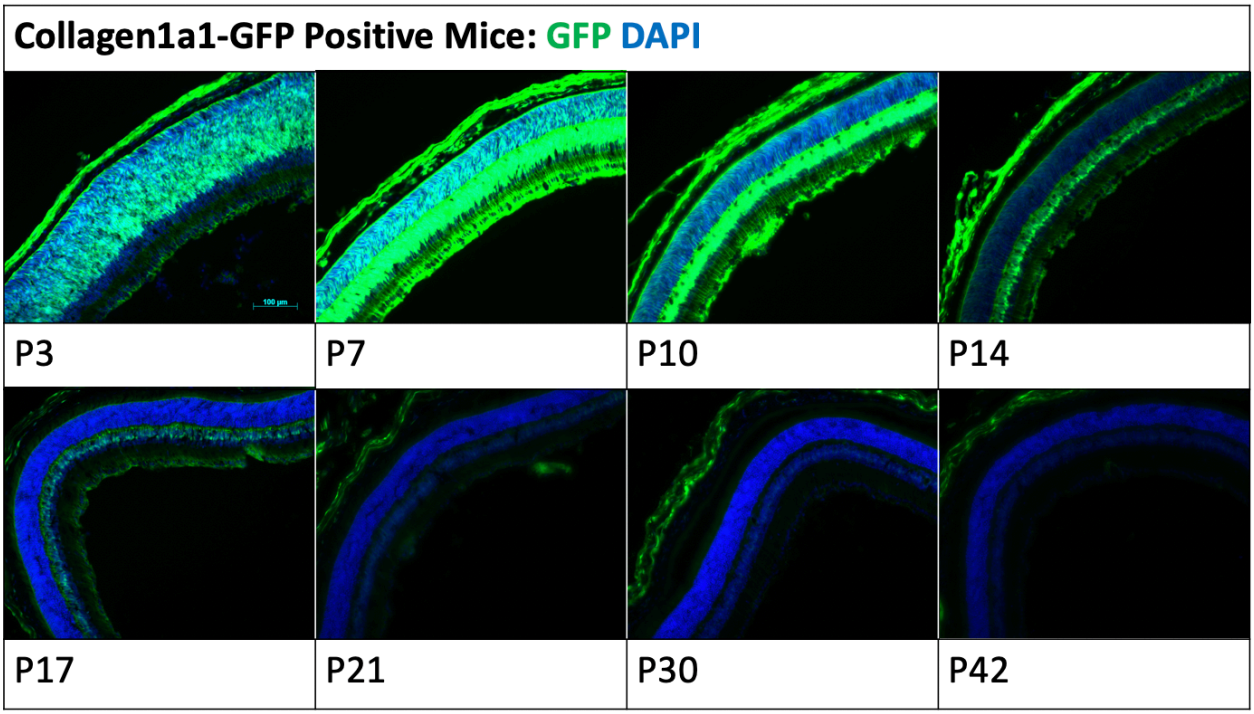

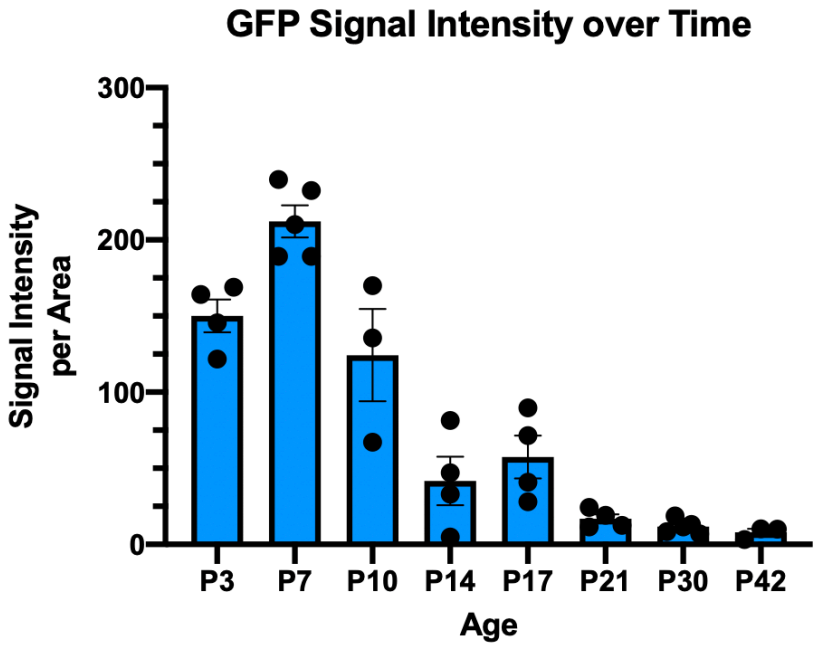

Figure 1: Collagen1a1-GFP expression at various postnatal timepoints in healthy mice. GFP expression increases from P3 to P7, then decreases precipitously with time. All mice retinas are 10µm thick and had an exposure time for GFP and DAPI at 100ms and 0.8ms respectively. Scale bar is 100µm. Error bars represent one SEM.

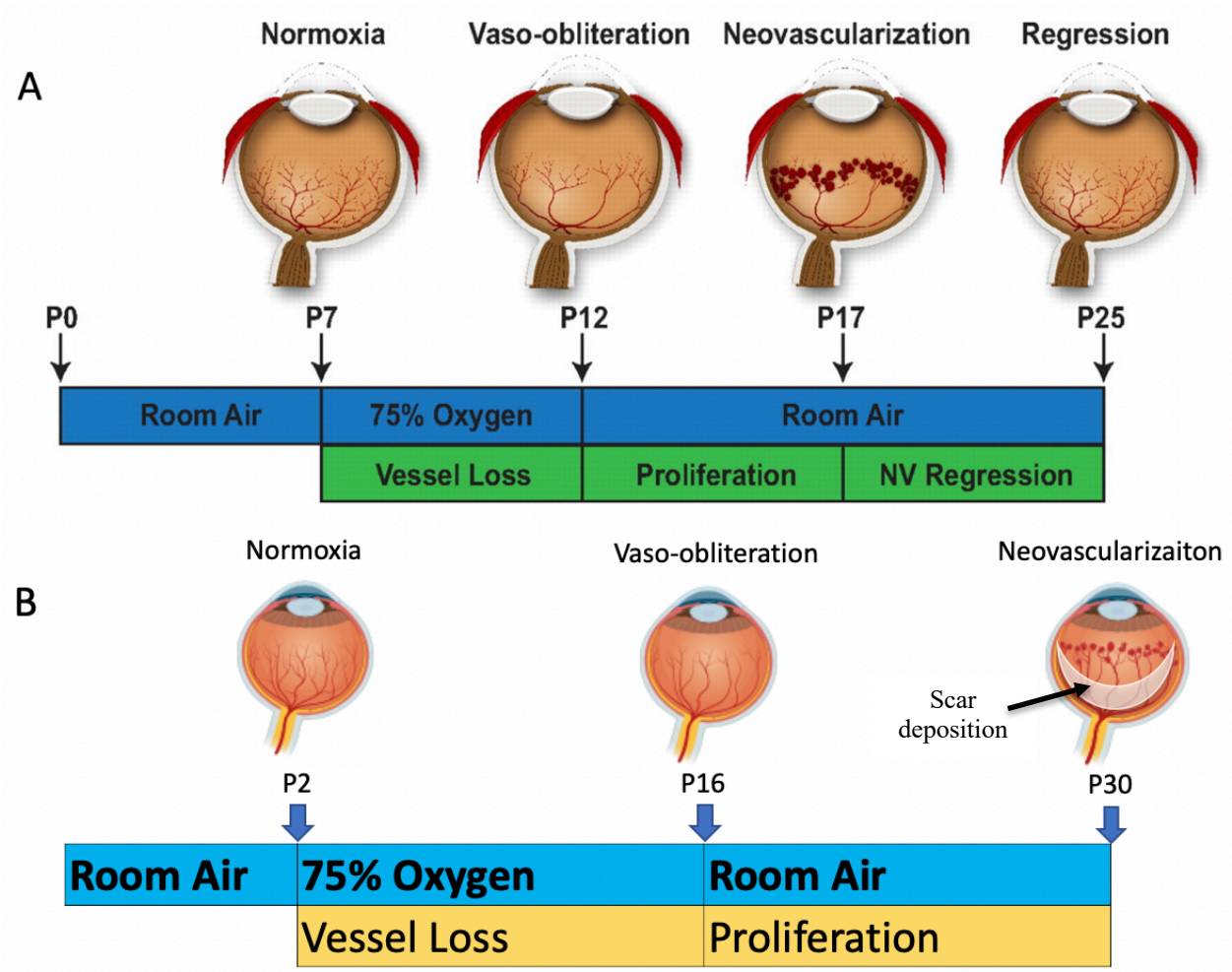

Figure 2: Comparison between LOIR and traditional OIR protocols. (A) This is the protocol schematic for the "Smith" model of Oxygen Induced Retinopathy (OIR) taken from Connor, K. *et. al* [21]**.** (A) This is a protocol schematic for OIR. We take postnatal day 7 (P7) mice from room air, which is at an atmospheric oxygen concentration of 21%, and place them in a 75% oxygen content chamber for 5 days. We remove these P12 mice from the high oxygen content and place them back in room air. The schematic also outlines when the retinal vasculature is normoxic, vaso-obliterated, neovascularized, and regressed (or recovered). (B) This is the protocol schematic for Long Oxygen Induced Retinopathy (LOIR) model. This model is based on the "Smith" OIR model for ischemic retinopathies [16], and the schematic is based on Connor, K.'s *et. al.* illustration for the "Smith" OIR model [21]. This model has not been characterized beyond P30, and thus we do not see the regression phase of the model traditionally seen in mice at later timepoints of OIR pathology. However, it is based on the idea that since younger premature babies that undergo oxygen treatment, and the longer the oxygen treatment is, have a higher chance of developing ROP, we placed younger mice in the oxygen chamber for a longer duration to get the pathology we observe in this model.

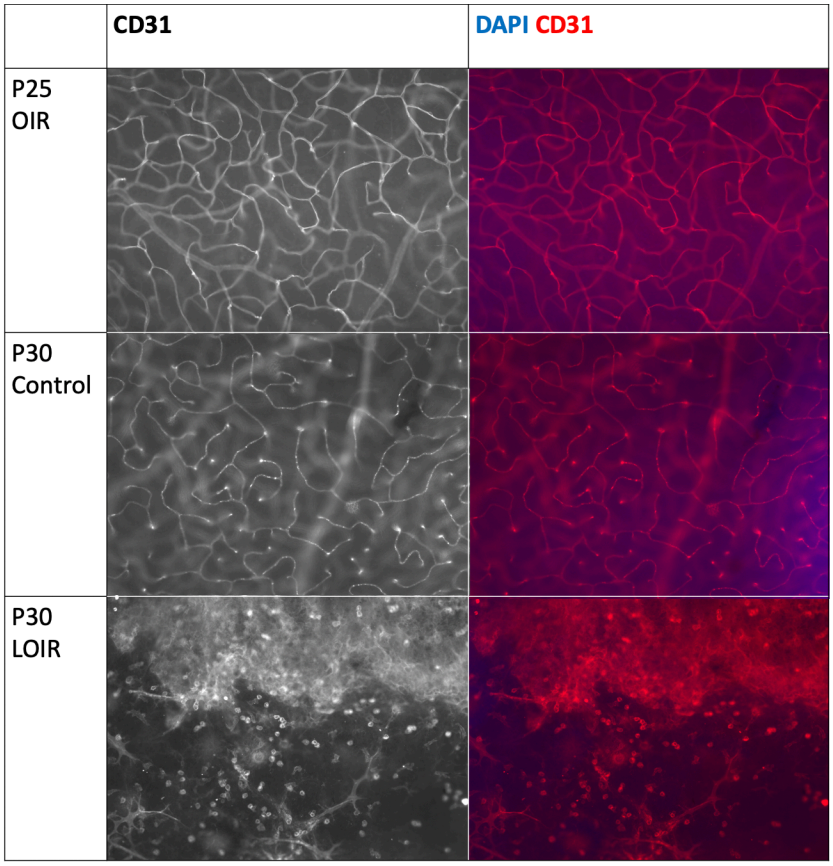

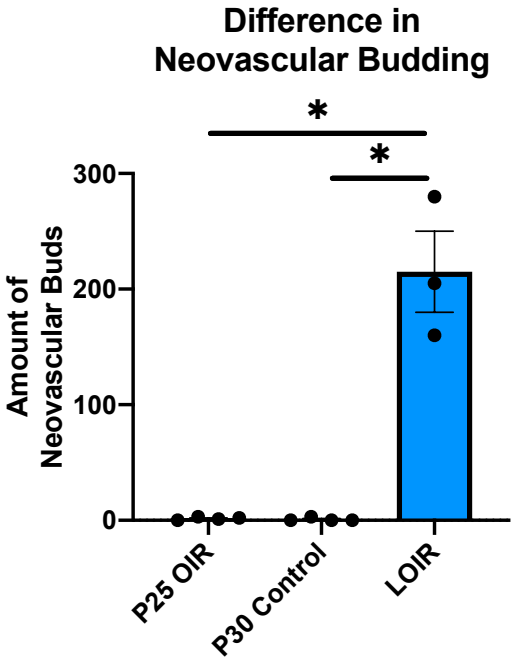

Figure 3: Vascular comparison between LOIR mice retinas to P25 traditional OIR mice and LOIR age matched controls. As we can see in the LOIR flatmounted retina, we have the formation of neovascular buds, pathology found in ROP and OIR retinas when new vasculature is developing. In both controls, we have normal vasculature development lacking these buds. It is important to note that P25 OIR control retinas did have neovascular budding at an earlier timepoint, however, these retinas recover proper vasculature by P25.
*$p<0.05$

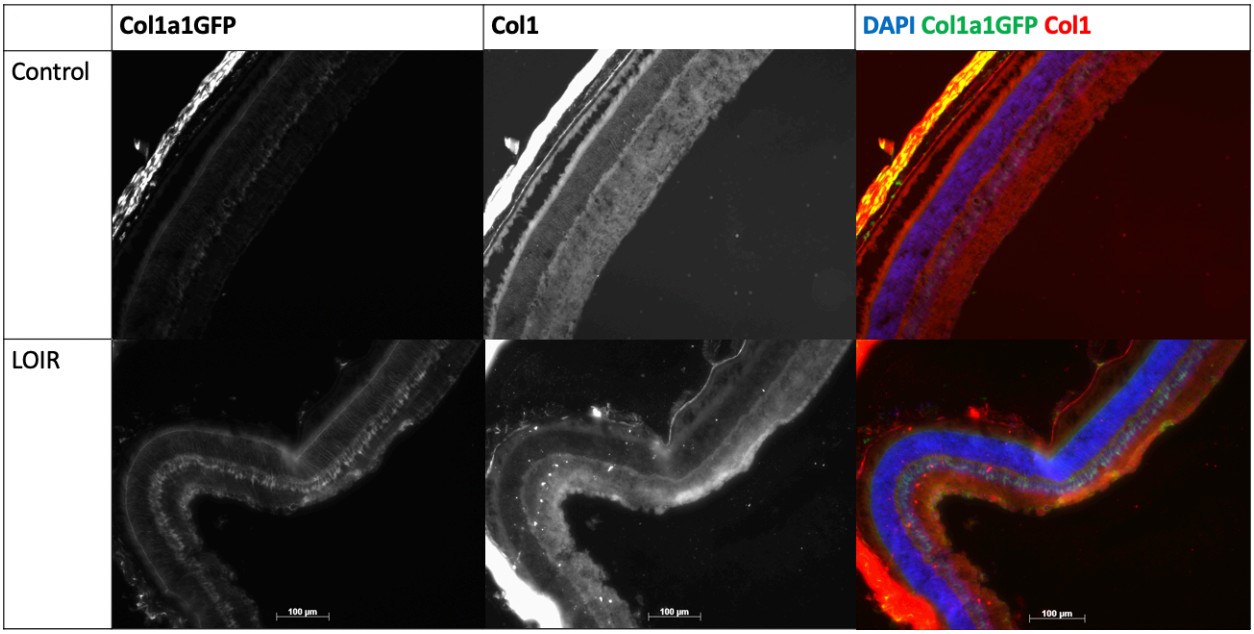

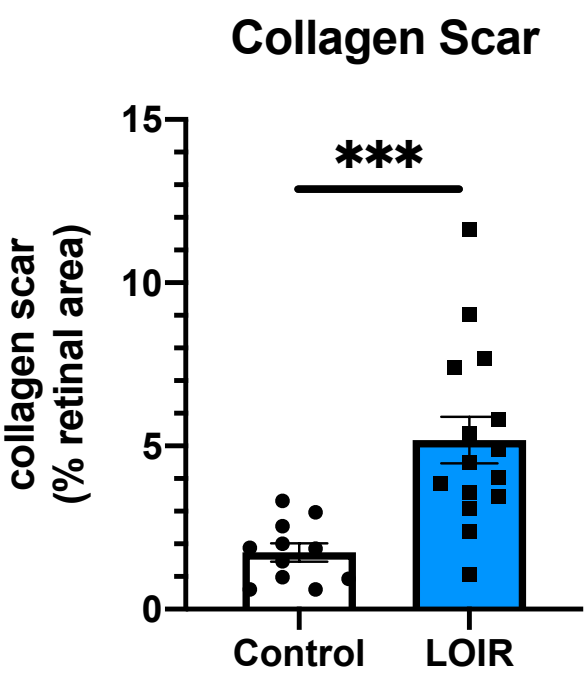

Figure 4: Collagen scar pathology in LOIR retinas. Fixed and dissected Collagen1a1-GFP positive retinas were stained and imaged after dissection under a microscope to visualize GFP+ cells and collagen 1 protein deposition. Both LOIR and control mouse sections express GFP, however there is significantly more collagen 1 protein deposition in the LOIR retinas relative to control retinas. Scale bar is 100µm.

***p<0.0001

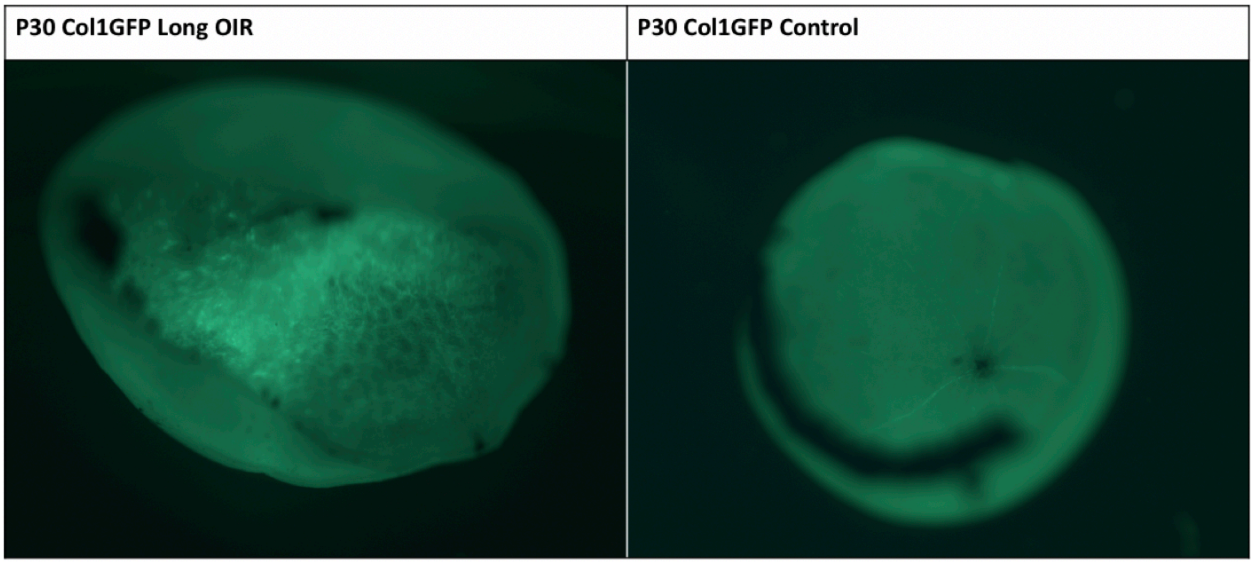

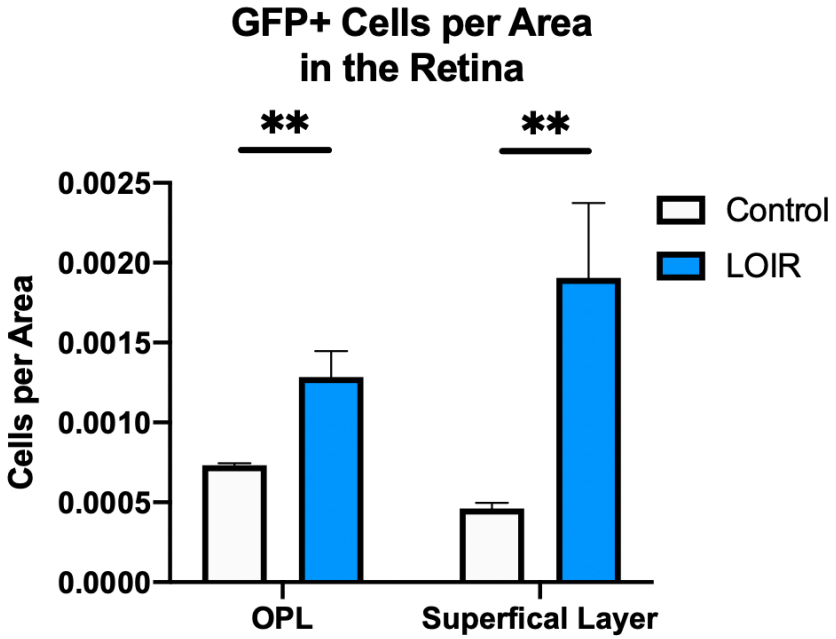

Figure 5: Collagen1a1-GFP positive cells per area in the Outer Plexiform and Superficial Layers of the retina. We see in whole retinas that there seems to be more expression of GFP positive cells. We sectioned LOIR and control retinas and quantified GFP positive cells in the Outer Plexiform and Superficial Layers. We found that there are significantly more GFP positive cells per area in both areas analyzed in LOIR mice. Error bars signify SEM. Images used for analysis had the same exposure time for each color channel.

**$p<0.01$

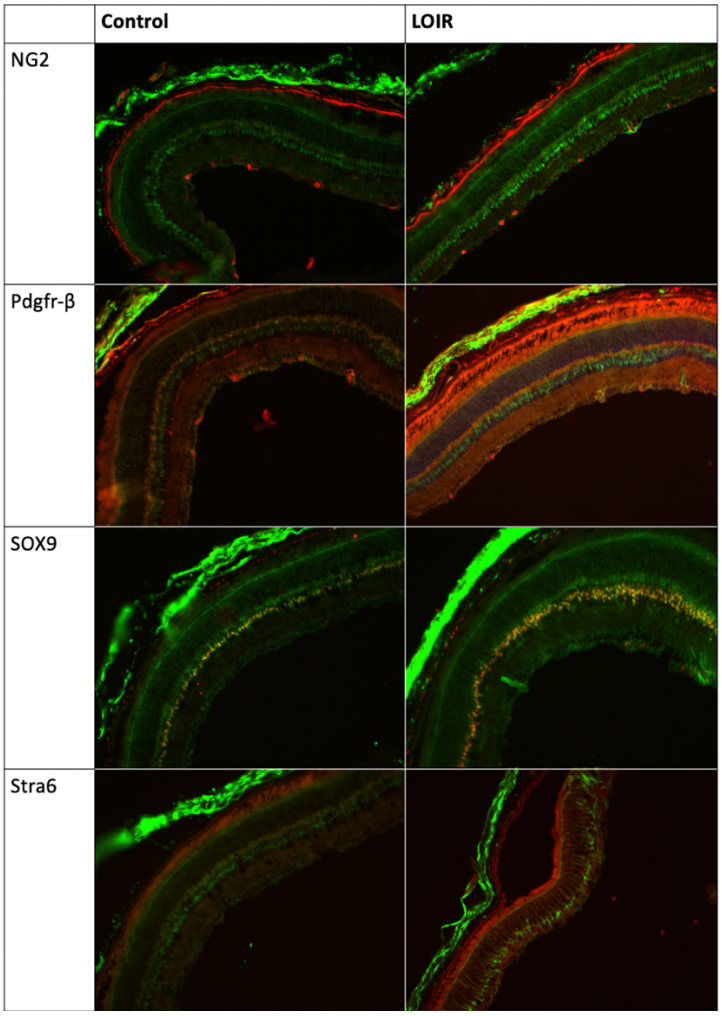

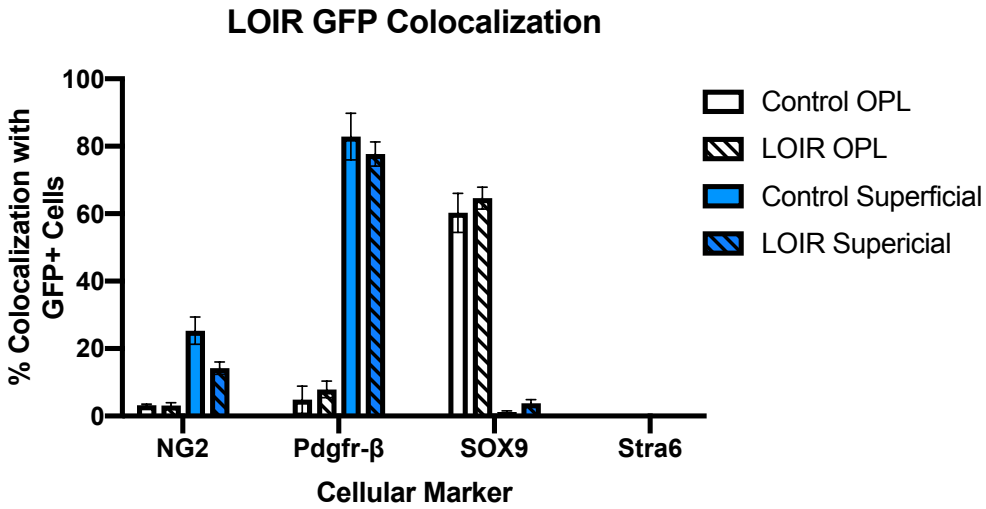

Figure 6: Colocalization of various cellular markers with GFP positive cells in LOIR retinal sections. Here we stained for a pericyte markers (NG2), a fibroblast marker (Pdgfr-β), a Müller glia marker (SOX9), and a retinal pigment epithelium marker (Stra6). After quantification of colocalization, we see the majority of GFP positive cells are SOX9 positive, however, the majority of superficial GFP positive cells colocalize with Pdgfr-β or NG2, suggesting surface collagen 1 producing cells originate from pericytes, and the majority of collagen 1 production in the deeper layers originate from Müller glia.

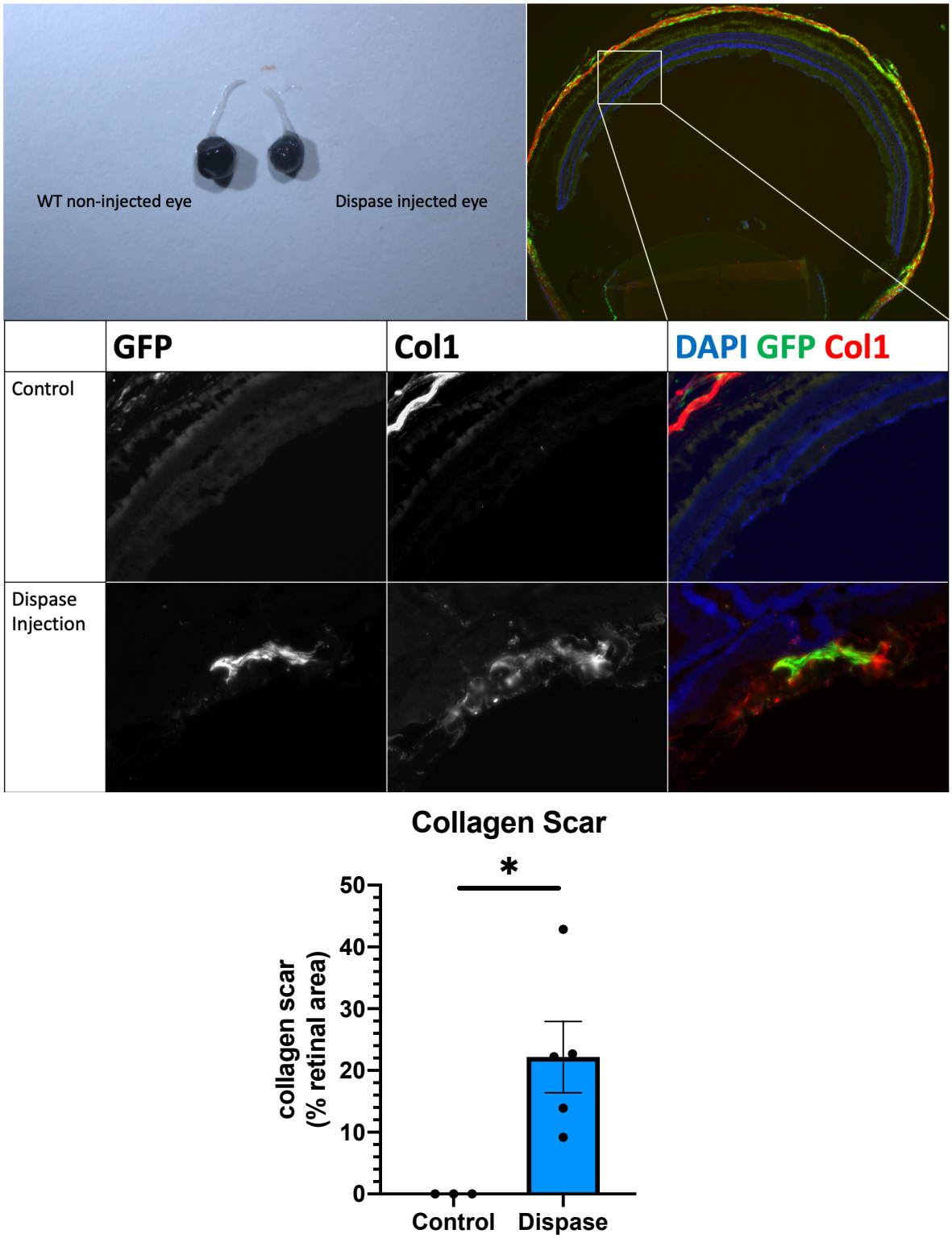

Figure 7: Collagen scar pathology in dispase injected retinas. Fixed and dissected Collagen1a1-GFP positive retinas were stained and imaged after dissection under a microscope to visualize GFP+ cells and collagen 1 protein deposition. There is more GFP expression and significantly more collagen 1 deposition in dispase injected mice relative to non-injected controls.
*$p<0.05$

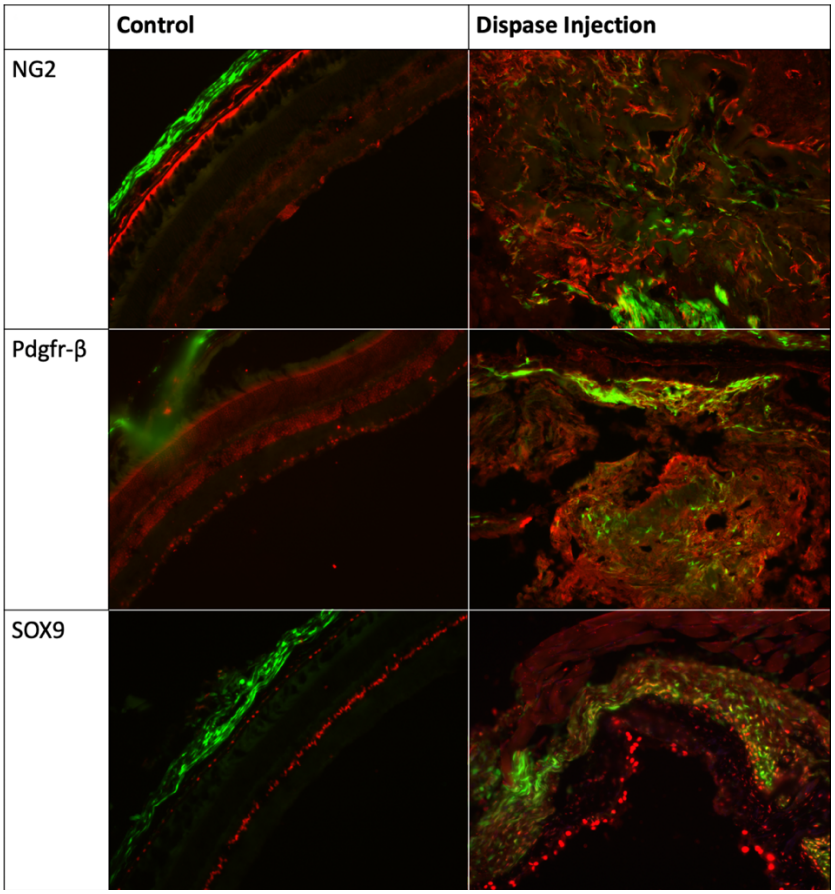

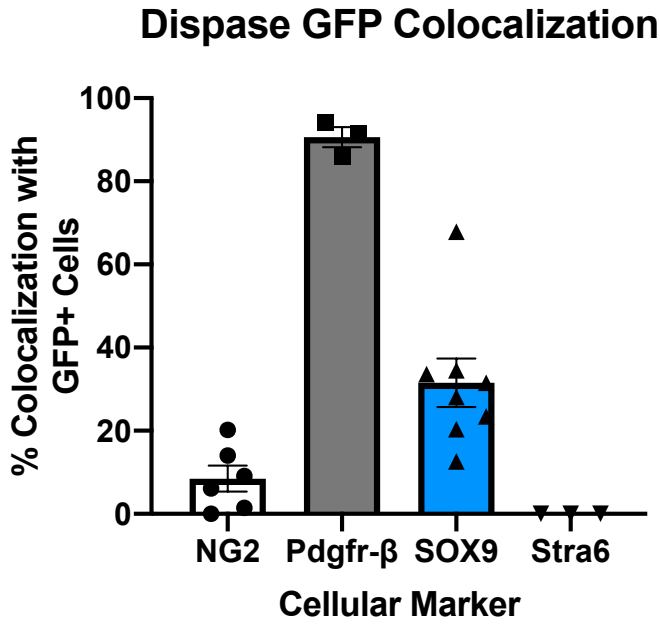

Figure 8: Colocalization of various cellular markers with GFP positive cells in dispase injected retinal sections. Here we stained for a pericyte markers (NG2), a fibroblast marker (Pdgfr-β), a Müller glia marker (SOX9), and a retinal pigment epithelium marker (Stra6). After quantification of colocalization, we see the majority of GFP positive cells are also Pdgfr-β positive. We do not see GFP positive cells in the retina of controls since these are adult mice, and collagen 1 expression at this age in the retina is very low. However, you can still see expression in the sclera in these controls.

GFP expression over time in control retinas. To determine if long OIR and dispase injection models human scarring pathology, we obtained Collagen1a1-GFP mice that express GFP under the control of the collagen 1 promoter. Collagen 1 is a key marker for fibrotic scarring; therefore, we can use GFP as a reporter for collagen 1 protein production which may suggest the production of a fibrotic scar. With these mice, we collected fixed retinas at various prenatal time points shown in figure 1 and characterized GFP expression in the mouse retina over time. Quantifying GFP fluorescence intensity gave us a baseline for collagen 1 expression in the retina. As seen in figure 1, the development of retina is apparent where the layers of the retina become more distinct over the first 10 postnatal days. Overall, GFP expression increases until P7, then declines precipitously over time in the mouse retina, suggesting collagen 1 protein production decreases in non-disease retinas over the course of time.

Neovascularization is present in P30 mice that experienced LOIR. To see the effect of LOIR on vascular development in the mouse retina, we performed LOIR on Collagen1a1-GFP positive mice, performed traditional OIR on a wild type mouse, and left Collagen1a1-GFP positive mice in a normoxic environment. We fixed the retinas from these mice, stained for blood vessels, flatmounted the retinas, and imaged them. As seen in figure 3, in both P25 OIR and normoxic P30 controls, the retina's vasculature has proper development and lacks neovascular buds. P25 OIR mice have recovered from previous vaso-obliteration and neovascularization events known to develop from this model [16,18-19,21-22]. P30 LOIR mice, however, are experiencing neovascularization. We also commonly observed blood in the retinal tissue, although we did not image this, suggesting another common pathology of ischemic retinal diseases. This suggests that

the LOIR model causes more severe pathology in mice retinas since at this time point are still avascular and undergoing neovascularization.

Scar production increases in long OIR mouse retinas. To determine if the long OIR model produces scar tissue on the mouse retina, we imaged fixed Collagen1a1-GFP mice retinas, sectioned the retinas, and stained for Collagen 1 protein, a protein present in fibrotic scars (Figure 4). Here, we see collagen 1 deposition on the superficial layer of the retina surrounding GFP positive cells throughout the long OIR retinas. After quantification, we see that in LOIR mice retinas, there is significantly more collagen 1 deposition per area relative to controls. This suggests LOIR induces scar production in the retina, and further models a more severe pathology compared to traditional OIR.

GFP expression increases in the LOIR mouse model. To see the effect of LOIR on GFP expression in the mouse retina, we fixed and sectioned LOIR and control mice retinas, stained, and imaged them to quantify amount of GFP cells in the superficial layer and the Outer Plexiform layer. As we see in figure 5, GFP expression significantly increase in both layers in long OIR retinas relative to same age normoxic controls. This suggests LOIR induces an increased production of collagen 1 protein.

Pericyte, Fibroblast and Müller glia markers colocalize with GFP positive cells in LOIR retinas. To observe what cell specific markers colocalized with GFP positive cells, we immunostained for a pericyte marker (NG2), a fibroblast marker (Pdgfr-β without NG2), a Müller glia marker (SOX9), and a retinal pigment epithelium marker (Stra6). These markers are of interest

to us, since past studies suggest both retinal pigment epithelial cells and Müller glia to produce scar tissue [10-12], and in peripheral tissues, it is known that fibroblasts produce fibrotic scars and pericytes aid in angiogenesis which is a driving factor for retinal scarring in ROP [5,7]. In figure 6, we see that the majority of Outer Plexiform layer GFP positive cells colocalize with the Müller glia marker, and the majority of superficial layer GFP positive cells colocalize with pericyte and fibroblast markers. This suggests that collagen 1 scar tissue formed on the surface of the retina may originate from fibroblast or pericytes, while collagen 1 scar tissue in deeper retinal layers may originate from Müller glia.

Dispase injections cause scar deposition in mouse retinas. To determine the morphological effect of intravitreal dispase injections, we imaged whole mouse eyes that were injected. In figure 6, we see that dispase injections cause morphological changes that lead to a shrunken eye, which is comparable to the human disease phthisis bulbi. To see if these injections have an effect on fibrotic scar formation, we sectioned injected eyes and non-injected controls, and stained for collagen 1 protein. We quantified collagen deposition per retinal area, and as we see in figure 7, collagen 1 expression significantly increases in the dispase injected retinas relative to the non-injected control eyes. Furthermore, we can visually see a significant increase in GFP expression since the control eyes are not expressing GFP at all in the retina, yet we see GFP expression in the dispase injected retina. This suggests the dispase injection models scarring pathology in the mouse retina that is similar to the pathology of phthisis.

Pericyte, Fibroblast and Müller glia markers colocalize with GFP positive cells in dispase injected retinas. To observe what cell specific markers colocalized with GFP positive

cells, we immunostained for a pericyte specific marker (NG2), a fibroblast and pericyte marker (Pdgfr-β), a Müller glia marker (SOX9), and a retinal pigment epithelium marker (Stra6). In figure 8, we do not see GFP expression in non-injected control eyes, hence we do not see any colocalization in control retina. In dispase injected retinas, we see we the majority of GFP positive cells colocalize with the fibroblast marker. This suggests that collagen 1 scar tissue deposition is produced my mainly fibroblasts in this dispase injection model. Müller glia and a small portion of pericytes also colocalize with GFP positive cells, suggesting the possibility that all three of these cell types play a role in scar production in the retina in this model.

Discussion

Collagen1a1-GFP signal decreases over time. With the various images at different prenatal timepoints in normoxic retinas, we see the development of GFP positive cells. In figure 1, early in development, the majority of retinal tissue is GFP positive, showing that the majority of the deep and middle areas of the retina in early stages of development produces collagen 1. As the mice get older, less overall area of the retina is GFP positive, and there is a decrease in GFP expression. The GFP positive cells in the process seem to organize to the middle and surface layers of the retina. This may indicate that younger pups are more vulnerable to the production of scarring since there is larger collagen expression in both cells and intensity at younger ages. Or possibly that there is a "Goldilocks zone" where pathology will only be expressed if the mice are at a particular age of relatively high levels of collagen expression with organization of those collagen expressing cells tending to be in the middle and surface layers, such as P10 and P17 in figure 1. Repeating LOIR experiments at an older age in mice may be interesting to perform to see if we obtain reduced scarring pathology.

Long OIR is a reliable and repeatable scarring model for Retinopathy of Prematurity in mice. Long OIR is a more severe model for Retinopathy of Prematurity that we developed based on the traditional OIR model [16,18]. We have repeated this model successfully with the same pathologies of neovascular budding and a plaque-like scar forming on the surface of the retina at postnatal day 30 that is akin to a retinal scar (figures 3-5). Also, LOIR does not recover from either vascular or scarring pathology at this timepoint. The LOIR model more closely resembles ischemic retinal diseases like ROP due to prevalent neovascularization at this later timepoint without

recovery, and the production of scar tissue, making LOIR a good model for later stages of ROP where abnormal blood vessels and retinal scar tissue development lead to retinal detachment.

In LOIR, GFP expression increases relative to normoxic controls, and scar tissue formation in LOIR retinas surround GFP positive cells, suggesting that these cells are the origin of the scar (figure 4 and 5). Using this newly developed scarring model, we can study the cellular mechanisms of retinal fibrotic scarring and the origins of this scar during disease. In the future, we will use fluorescence-activated cell sorting (FACS) to separate GFP positive cells and perform RNA sequencing to determine the cell type of origin for retinal scar tissue and the cellular mechanisms behind this scar formation.

As stated before, we were interested in seeing what cellular markers colocalize with GFP positive cells in LOIR. Fibroblasts are known to lead to scar deposition in peripheral tissues after injury, making this cell type of interest to us to see if this is the cell that forms scars in the retina. Pericytes are known to help blood vessels develop when they undergo angiogenesis, so we were also interested in this particular cell [5,7]. And, as stated before, both Müller glia and RPE have been noted in the literature to produce scar tissue in the retina [10-12, 23-24]. Therefore, stained for pericytes, fibroblasts, Müller glia, and RPE markers in the retina to see if these cells are also expressing collagen 1 protein with GFP as the reporter protein for this activity. Interestingly, what we see is colocalization of different cell specific markers in different areas of the retina. On the superficial layer of the retina, we mainly see colocalization both Pdgfr-β and NG2, where together they are markers for pericytes, GFP positive cells, suggesting pericytes are the main scar producing cell on the superficial area of the retina. It also may suggest both pericytes and fibroblast are present and producing scar tissue in the retina. In deeper layers, however, we mainly see

colocalization of Müller glia markers, suggesting Müller glia as the main scar producing cell in deeper layers of the retina.

However, these scar producing events may not be mutually exclusive. Previous studies imply that Müller cells play a factor in forming scars in the retina, commonly referred to as gliosis [12,23-24]. These studies suggest that Müller glia undergo hypertrophic growth in disease and extend their glial processes to the surface of the retina and deposit scar tissue. If this is the case, both Müller glia and pericytes may contribute to the formation of scars in the retina rather than one cell type over the other.

Issues arise with the maintenance of mice in this model (figure 2b). Every 48 hours for two weeks, it is necessary to switch the nursing mom in the 75% oxygen chamber with a nursing mom in a normoxic environment, ideally from the age-matched littermate control cage. We have experienced that switching less frequently has led to the increase in chance of death of the nursing moms from oxygen toxicity. This issue also leads us to question the amount of times nursing mice can be exposed to the long OIR experiment. Prolonged oxygen exposure is toxic and can lead to a plethora of major diseases and disorders, therefore, we used a new litter from new nursing mice each time this experiment was repeated to avoid the issue of the nursing mom's premature death from prolonged oxygen exposure [22]. Furthermore, since oxygen exposure also may cause harm on mother mouse, there may be reciprocal harm to the next litter born from that mother mouse. Again, this raises the question of how many times a mother mouse can experience long OIR, not only for its own health, but also for the health of the following litter. Therefore, repeated long OIR exposure to mother mice may increase variability of the resulting scarring phenotypes, gene expression, and increase the chance of death for the nursing pups.

Also, mice used in these experiments were derived from C57BL/6N vendor lines which can be positive for retinal degeneration mutations in the Cbr1-1 gene [25]. The mice used for the quantifications were not genotyped for this recessive mutation prior to the analysis, so the resulting observed phenotypes may be due to the retina degeneration mutation rather than the long OIR model or dispase injections. We have since found that many of our mating pairs consist of 2 mice heterozygous for the mutation, so the pups have a 25% chance of having 2 copies. However, all of the pups analyzed had retinal scarring, yet only 25% get the retinal degeneration gene. Furthermore, we also tested on non-LOIR mice and these mice do not develop a scar, suggesting the gene alone does not lead to the phenotypes we have observed. We will repeat the experiments with mice without 2 copies of the mutation to confidently conclude that GFP expression increases in these disease models.

Dispase injection causes scarring but the model needs to be better optimized for future use. Dispase injections are commonly used in rabbits as a model of proliferative vitreoretinopathy [15]. We repeated injections in multiple mice, however, there were varying phenotypic results that made both quantifying cells and RNA sequencing difficult. Although we used the same amount of injected dispase for each mouse, the eyes throughout the course of time would degrade at different rates, causing some injected eyes to shrink and shrivel more than others. The amount of degradation that occurs also made it difficult for the retina to be cleanly dissected and usable for RNA sequencing. The pathology, however, of dispase injections that we observed is akin to *phthisis bulbi*, a disease that is usually caused by physical injury to the eye that leads to progressive degradation of the whole eye (figure 7 and 8). Dispase acts like an injury and progressively degrades the eye and retina over time, as shown in figures 6 and 7. After our

quantification, we saw similar colocalization results to LOIR. Pdgfrβ and SOX9 were the top two cellular markers that colocalized with GFP, suggesting fibroblasts and/or Müller glia deposit scar tissue in the eye (figure 8). Because there is slight colocalization of GFP positive cells will NG2, pericytes may be present producing scar tissue rather than fibroblasts.

An issue of the dispase model is its non-specificity. Dispase hydrolyzes N-terminal peptide bonds of non-polar amino acid residues, which includes to a small extent collagen 1. This confounds our analysis of visualizing collagen scarring in the retina after the disease. However, this does not affect collagen expression, and therefore, GFP expression, thus still allowing for colocalization experiments to be valid and RNA sequencing to progress if it is further optimized. This model could be further optimized by decreasing the amount of dispase injected or shortening the duration after injection to reduce the extent of degradation. With less degradation, retinal dissections may be easier to accomplish for RNA sequencing in order to determine what cell scar tissue originates from.

References

[1] Wynn, T.A. Cellular and molecular mechanisms of fibrosis. (January 2008). *J Pathol*; 214(2): 199–210.

[2] Martin, P., Nunan, R. (July 2015). Cellular and molecular mechanisms of repair in acute and chronic wound healing. *British Journal of Dermatology*; 173(2); 370-378.

[3] Bataller, R; Brenner, DA. (February 2005). Liver fibrosis. Journal of Clinical Investigation; 115(2): 209-218.

[4] Toosi, A. (December 2015). Liver Fibrosis: Causes and Methods of Assessment, A Review. *Romanian Journal of Internal Medicine*; 53(4): 304-314

[5] Kumar A., Mohanraj S.N., Duraipandi K., Pai A.V. (2016). Antiangiogenic Agents and Photodynamic Therapy. Velpandian T. *Pharmacology of Ocular Therapeutics*; Adis, Cham; 245-268.

[6] Cho, C., Wang, Y., Smallwood, P., Williams, J., Nathans, J., (May 2019). Dlg1 activates beta-catenin signaling to regulate retinal angiogenesis and the blood-retina and blood-brain barriers. *eLife* 8e45542: doi:10.7554/eLife.45542.

[7] Semenza, Gregg L. (2013). Oxygen Sensing, Hypoxia-Inducible Factors, and Disease Pathophysiology Annual Review of Pathology. *Mechanisms of Disease*; 9:47-71.

[8] Tosi, G. M., Marigliani, D., Romeo, N., & Toti, P. (2014). Disease Pathways in Proliferative Vitreoretinopathy: An Ongoing Challenge. *Journal of Cellular Physiology*; 229(11): 1577–1583.

[9] Trojanowska, M., LeRoy, E., Eckes, B., Krieg, T. (1998). Pathogenesis of fibrosis: type 1 collagen and the skin. *J Mol Med;* 76: 266–274.

[10] Hiscott, P., Sheridan, C., Magee, R., Grierson, I. (1999). Matrix and the retinal pigment epithelium in proliferative retinal disease. *Progress in Retinal Eye Research;* 18(2), 167-190.

[11] Machemer, R., Horn, D., Aaberg, T. (February 1978). Pigment Epithelial Proliferation in Human Retinal Detachment with Massive Perinatal. *Am J Ophthalmol*; 85(2): 181-91.

[12] Friedlander, Martin. Fibrosis and diseases of the eye. (March 2007). *J Clin Invest*. 1; 117(3): 576–586.

[13] Eming, S., Krieg, T. and Davidson, J. (2007). Inflammation in Wound Repair: Molecular and Cellular Mechanisms. *Journal of Investigative Dermatology;*127(3): 514-525.

[14] Frenzel, E., Neely, K., Walsh, A., Cameron, J., Gregerson, D. (October 1998). A New Model of Proliferative Vitreoretinopathy. *Investigative Ophthalmology & Visual Science*; 39: 2157-2164.

[15] Agrawal, R., He, S., Spee, C., Cui, J., Ryan, S., Hinton, D. (February 2007). In vivo models of proliferative vitreoretinopathy. *Nature Protocols*; 2: 67–7.

[16] Smith, L., Wesolowski, E., McLellan, A., Kostyk, S., D'Amato, R., Sullivan, R., D'Amore, P. (1994). Oxygen-induced retinopathy in the mouse. *Invest Ophthalmol Vis Sci*.; 35: 101-111.

[17] Alon, T., Hemo, I., Tin, A., Pe'er, J., Stone, J., Keshet, E. (October 1995). Vascular endothelial growth factor acts as a survival factor for newly formed retinal vessels and has implications for retinopathy of prematurity. *Nature Medicine;* 1(10): 1024-1028.

[18] Selvam, S., Kumarc, T., Fruttigera, M. (March 2018). Retinal vasculature development in health and disease. *Progress in Retinal and Eye Research*; 63(2), 167-190.

[19] Lajko, M., Cardona, H., Taylor, J., Shah, R., Farrow, K., Fawzi, A. (November 2016). Hyperoxia-Induced Proliferative Retinopathy: Early Interruption of Retinal Vascular Development with Severe and Irreversible Neurovascular Disruption. *Public Library of Science One*; 11(11): e0166886, doi:10.1371/journal. pone.0166886.

[20] Schneider, C. A.; Rasband, W. S. & Eliceiri, K. W. (2012). "NIH Image to ImageJ: 25 years of image analysis." *Nature methods* 9(7): 671-675.

[21] Connor, K., Krah, M., Dennison, R., Aderman, C., Chen, J., Guerin, K., Sapieha, P., Stahl, A., Willett, K. & Smith, L. (October 2009). Quantification of oxygen-induced retinopathy in the mouse: a model of vessel loss, vessel regrowth and pathological angiogenesis. *Nature Protocols*; 4: 1565–1573.

[22] Uttara, B., Singh, A., Zamboni, P. and Mahajan, R.T. (March 2009). Oxidative Stress and Neurodegenerative Diseases: A Review of Upstream and Downstream Antioxidant Therapeutic Options. *Current Neuropharmacology*; 7(1): 65-74.

[23] Bringmann, A., Iandiev, I., Pannicke, T., Wurm, A., Hollborn, M., Weidemann, P., Osborne, N., Reichenbach, A. (2009). Cellular signaling and factors involved in Müller cell gliosis: Neuroprotective and detrimental effects. *Progress in Retinal and Eye Research*; 28(6): 423-451.

[24] Bringmann, A., Pannicke, T., Grosche, J., Francke, M., Wiedemann, P., Skatchkov. S., Osborne, N., Reichenbach, A. (July 2006). Müller cells in the healthy and diseased retina. *Progress in Retinal and Eye Research*; 25(4): 397-424.

[25] Mattapallil, M., Wawrousek, E., Chan, C., Zhao, H., Roychoudhury, J., Ferguson, T., Caspi, R. (May 2012). The Rd8 mutation of the Crb1 gene is present in vendor lines of C57BL/6N mice and embryonic stem cells, and confounds ocular induced mutant phenotypes. *Invest Ophthalmol Vis Sci.;* 53(6): 2921-7. doi: 10.1167/iovs.12-9662.